Journal of Hazardous Materials 419 (2021) 126396

Contents lists available at ScienceDirect

Journal of Hazardous Materials

journal homepage: www.elsevier.com/locate/jhazmat

# Microplastics contamination in pearl-farming lagoons of French Polynesia

Tony Gardon [a,*,1], Maria El Rakwe [b], Ika Paul-Pont [c], Jérémy Le Luyer [a], Léna Thomas [b], Enora Prado [b], Kada Boukerma [b], Anne-Laure Cassone [c], Virgile Quillien [a], Claude Soyez [a], Louis Costes [a], Margaux Crusot [d], Catherine Dreanno [b], Gilles Le Moullac [a], Arnaud Huvet [c]

[a] Ifremer, ILM, IRD, Univ Polynésie française, EIO, F-98719 Taravao, Tahiti, Polynésie française, France
[b] Ifremer, Laboratoire Détection, Capteurs et Mesures (LDCM), Centre Bretagne, ZI de la Pointe du Diable, CS 10070, 29280 Plouzané, France
[c] Univ Brest, Ifremer, CNRS, IRD, LEMAR, F-29280 Plouzané, France
[d] Univ Polynésie française, Ifremer, ILM, IRD, EIO, F-98702 Faa'a, Tahiti, Polynésie française, France

ARTICLE INFO

Editor: Dr. R Teresa

*Keywords:*
Microplastics pollution
Atolls
Surface water
Water column
Pearl oyster

ABSTRACT

Pearl-farming is the second most important source of income in French Polynesia. However, tropical lagoons are fragile ecosystems with regard to anthropogenic pressures like plastic pollution, which threaten marine life and the pearl oyster-related economy. Here, we investigated the spatial distribution of microplastics (MP) and concentrations in surface water (SW), water column (WC) and cultivated pearl oyster (PO) from three pearl-farming atolls with low population and tourism. Microplastics were categorized by their size class, shape, colour and polymer type identified using FTIR spectroscopy. Widespread MP contamination was observed in every study site (SW, 0.2–8.4 MP $m^{-3}$; WC, 14.0–716.2 MP $m^{-3}$; PO, 2.1–125.0 MP $g^{-1}$ dry weight), with high contamination in the WC highlighting the need to study the vertical distribution of MP, especially as this compartment where PO are reared. A large presence of small (< 200 μm) and fragment-shaped (> 70%) MP suggests that they result from the breakdown of larger plastic debris. The most abundant polymer type was polyethylene in SW (34–39%), WC (24–32%), while in PO, polypropylene (14–20%) and polyethylene were more evenly distributed (9–21%). The most common MP identified as black-grey polyethylene and polypropylene matches the polymer and colour of ropes and collectors questioning a pearl-farming origin.

## 1. Introduction

Since the plastics industry first flourished in the 1950s, global plastic production has steadily increased, reaching 368 million tons in 2019 (PlasticsEurope, 2020). However, poor management of plastic waste means that it is frequently washed into the oceans, where it accumulates and disperses on a global scale, showing a great resilience (Thompson et al., 2004; Barnes et al., 2009). Studies estimate that the amount of plastic floating on the sea surface is between 93,000 and 236,000 tons, representing approximately 5000 to 50,000 billion fragments, 92% of which are microparticles of plastic (< 5 mm), also called "microplastics" (Eriksen et al., 2014; van Sebille et al., 2015). These microplastics (MP) can enter the marine environment by several pathways (reviewed in Andrady, 2011). The majority of MP found in the oceans are secondary MP (Lassen et al., 2015) produced by the fragmentation of larger plastic debris under a combination of environmental factors (physical, chemical and biological processes) (Andrady, 2011). Primary MP, in contrast, are those directly released into the environment as micro-sized particles (*e.g.* synthetic fibres, microbeads from the cosmetic industry, pre-production pellets or tire particles) (Boucher and Friot, 2017).

Microplastics have been reported in all major oceans and seas including the Pacific (Eriksen et al., 2013), Atlantic (Ivar do Sul and Costa, 2014) and Indian Oceans (Imhof et al., 2017), as well as the Southern Ocean (Isobe et al., 2017), Arctic polar waters (Lusher et al., 2015), Antarctica (Munari et al., 2017), and the Mediterranean (Collignon et al., 2012) and North Seas (Tamminga et al., 2018). They have been found everywhere, from populated coastal environments (Isobe et al., 2015; Frère et al., 2017) to the most remote areas (Obbard, 2018; Peeken et al., 2018). Their ubiquitous nature in all environmental matrices, from surface water (Eriksen et al., 2013; Lusher et al., 2015),

* Corresponding author.
*E-mail address:* tony.gardon@ifremer.fr (T. Gardon).
[1] Present address: PSL University, EPHE-UPVD-CNRS, USR 3278 CRIOBE, 98729 Moorea, French Polynesia & Laboratoire d'Excellence "CORAIL", Perpignan, France.

https://doi.org/10.1016/j.jhazmat.2021.126396
Received 12 April 2021; Received in revised form 2 June 2021; Accepted 10 June 2021
Available online 11 June 2021

down through the water column (Lattin et al., 2004) to the sediments (Van Cauwenberghe et al., 2013; Woodall et al., 2014), including in marine biota (Foekema et al., 2013; Cole et al., 2015), as their small sizes make them easily taken up by a wide range of organisms (Galloway et al., 2017).

In French Polynesia (FP), pearl-farming is the second most important economic activity, based on the trade of pearl and mother-of-pearl (IEOM, 2019). It also contributes to the social development of the territory by being widespread across 23 remote islands and atoll lagoons. However, pearl-farming is associated with a specific source of plastic pollution. The inventory carried out by Andréfouët et al. (2014) in the atoll lagoon of Ahe (FP) revealed thousands of tons of plastic pearl-farming gears (*e.g.* collectors, ropes, buoys or nylon ties). Rearing structures and equipment of these types (both derelict and operational) are accumulating over time in pearl-farming lagoons. They may fragment into smaller particles, which then add to MP entering the lagoons from other anthropogenic pressures and from the South Pacific subtropical gyre (Eriksen et al., 2013; Luna-Jorquera et al., 2019). This situation is worsened by the semi-enclosed environments of some of these lagoons, which could favour MP accumulation (Andréfouët et al., 2014). Pearl-farming could thus be causing a risk to itself through plastic pollution, with a potential impact of MP on the suspension filter-feeding pearl oyster *Pinctada margaritifera*. Indeed, exposure using polystyrene microbeads (6 and 10 μm) demonstrated a dose-dependent effect on the energy balance (Gardon et al., 2018) and dose-specific transcriptomic disruption to gene expression (Gardon et al., 2020) in *P. margaritifera*. However, these effects were only observed in experimental controlled conditions that do not properly represent the complexity of the environment. Furthermore, concentrations tested were not ecologically relevant since no environmental surveys had been performed in pearl-farming lagoons. To date, only one study has demonstrated the presence of MP in French Polynesia waters, using a 50 μm-plankton net in front of a public beach in Moorea, where they reached 0.74 MP $m^{-2}$ (Connors, 2017). There was, therefore, a strong need to evaluate and characterize MP pollution in pearl-farming lagoons.

The aim of the present study was to evaluate MP contamination in pearl-farming atoll lagoons of French Polynesia with low population and tourism. We investigated MP concentration, composition and spatial distribution in surface water (using a manta trawl, 335 μm-mesh) and the water column (using a planktonic net, 40 μm-mesh), as well as in the tissue of cultivated pearl oysters. Our study addressed two main aspects: (1) the distributions and concentrations of MP in the compartments investigated; (2) the identification of polymer types and relative abundance, in so far as the main characteristics of MP contamination could be related to those of local macroplastic pollution sources such as the widely distributed pearl-farming gears. The data produced should facilitate decision making for local government policies to assess and anticipate this emerging risk for pearl-farming sustainability in French Polynesia.

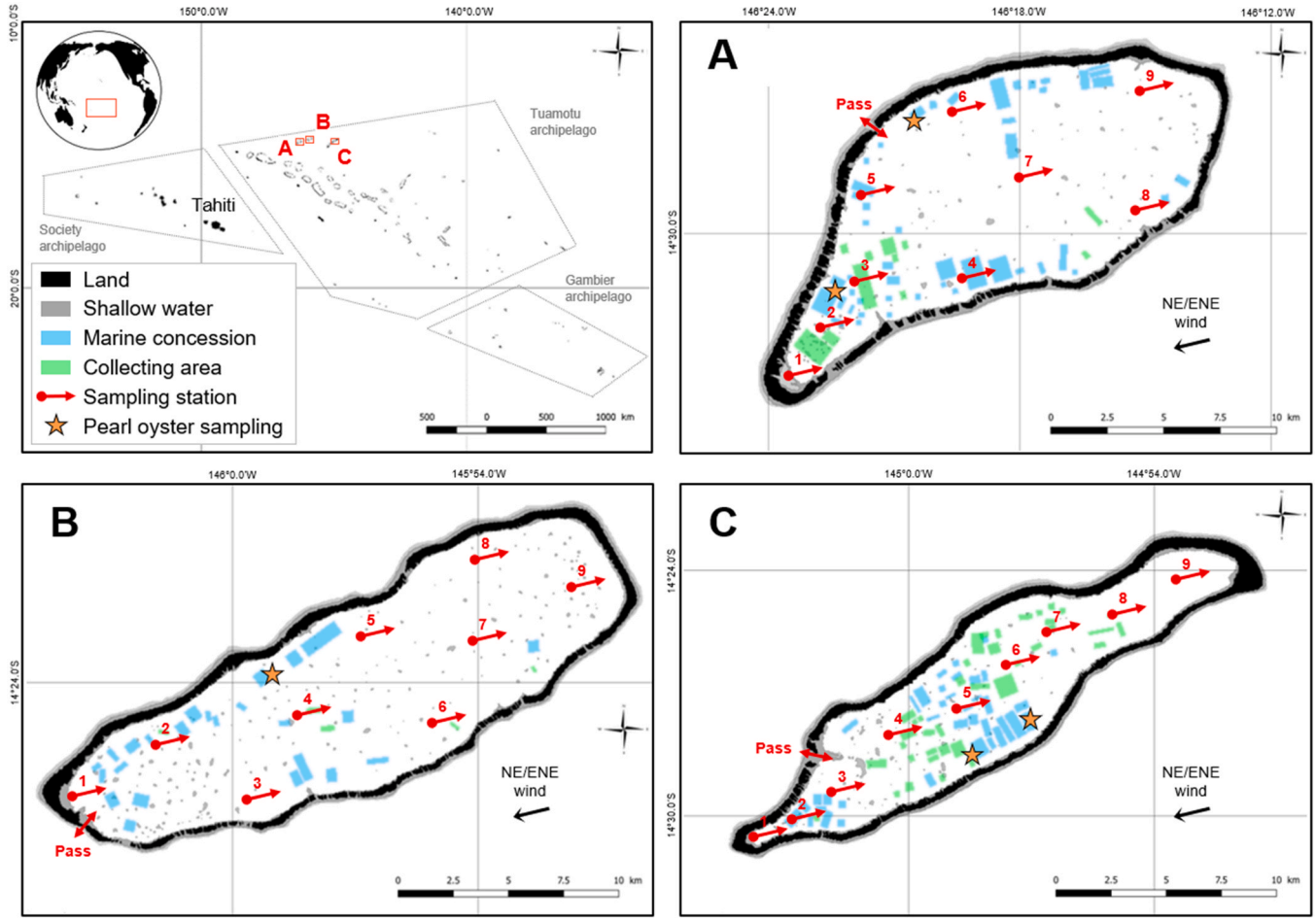


**Fig. 1.** Study site maps indicating pearl-farming activity and sampling locations in Ahe (A) Manihi (B) and Takaroa (C) atolls. Colours indicate land (black), shallow water (grey), pearl-farming marine concessions (blue) and spat-collecting areas (green). Red arrows and orange stars indicate sampling stations for seawater and pearl oysters, respectively. (For interpretation of the references to colour in this figure legend, the reader is referred to the web version of this article.)

## 2. Materials and methods

### 2.1. Study sites

Microplastics contamination was evaluated in three atoll lagoons (Ahe, Manihi and Takaroa) of Tuamotu archipelago (18° 47′ S, 141° 35′ W, FP), located to the north-east of Tahiti island (17° 40′ S, 149° 28′ W, FP). Sampling campaigns were carried out during the warm period in November 2017 in Takaroa (from 18 to 21th), and in March 2018 in Manihi (from 13 to 16th) and Ahe (from 17 to 20th) atolls. These study sites were chosen because of their pearl-farming activities which started in the 1980s. No particular event happened throughout history except in Takaroa, where the scale of pearl-farming (*i.e.* number of active pearl-farms) has declined since 2016 due to harmful algal bloom events that led to the death of many cultured oysters (Rodier et al., 2019).

Ahe (14° 30′ S, 146° 20′ W; Fig. 1A), Manihi (14° 24' S, 145° 57′ W; Fig. 1B) and Takaroa (14° 27′ S, 144° 58′ W; Fig. 1C) are semi-enclosed marine environments with 12, 13 and 20 $km^2$ of emerged land populated by 491 (41 inh./$km^2$), 650 (50 inh./$km^2$) and 674 (34 inh./$km^2$) inhabitants, respectively. Domestic wastewater is directly evacuated in the lagoon and/or in the ocean. No industrial area is established on these territories which are also marked by a low tourist activity, estimated at 4500 (Ahe), 4000 (Manihi) and 3500 (Takaroa) people in transit per year. The lagoons of Ahe (145 $km^2$), Manihi (165 $km^2$) and Takaroa (89 $km^2$) are each reached by a unique pass, which plays an important role in the water renewal, with about 34, 130 and 76 days of residence time, respectively (Pagès et al., 2001). In each location, specific areas are devoted to pearl-farming activities (*i.e.* maritime concessions for pearl oyster rearing) with additional collecting stations authorized by local government. Collecting stations are composed of spat collectors placed in specific zones of the atoll corresponding to optimal locations for spat settlement, notably based on hydrodynamic conditions (Thomas et al., 2016). Authorized surface areas for pearl-farming marine concessions are 831, 413 and 392 ha in Ahe, Manihi and Takaroa, representing 5.6%, 2.5% and 4.4% of the total lagoon areas, respectively. Additionally, 1536, 498 and 887 collecting stations are authorized in Ahe, Manihi and Takaroa, respectively (DRM, 2019). Ahe is currently the most productive pearl-farming atoll among study sites, followed by Mahihi and Takaroa with 884,743 (1.14 t), 307,757 (0.37 t) and 181,095 (0.20 t) reported produced pearls in 2019, respectively (DRM, 2019). A summary table of the study site characteristics is given in the Supplementary Information file (Table S1).

### 2.2. Seawater sampling

Lagoons being different for a large number of parameters (*e.g.* hydrodynamics, surface, demography, anthropogenic pressures) and sampling (time, number of farms, authorized marine concessions and collecting stations), their statistical comparison was not relevant. Our goal is rather a first mapping of MP contamination through nine sampling stations established in each lagoon, spread over the whole area. Vertical (water column) and horizontal (surface water) sampling of seawater was performed at each station. Two additional surface water samples were taken in the pass at each study site under conditions of inward and outward current flow (Fig. 1).

To study MP occurrence in the water column, a planktonic net with a 40 μm-mesh size and a circular opening of 0.4 m diameter was used for a vertical sampling. The net was weighted using a 1 kg lead weight in order to vertically sample from a vessel. The depth was measured with a graduated rope connected to the net wholly ranging from 8 to 54 m for the three study sites (detailed depths for each sampling location are given in Table S2). Once brought back on board, the net was thoroughly externally rinsed with *in situ* seawater to concentrate debris at the end of the net before purging the residual seawater into a hermetic glass jar. For the horizontal sampling, the top 20 cm of the sea surface microlayer was then sampled using a standard manta trawl with a 335 μm-mesh net and a rectangular net opening of 0.6 × 0.16 m, pulled at an average speed of two knots for 20 min. Sampling was systematically undertaken against the wind. A flow meter (model 23.091, KC Denmark Research Equipment and model 2030, General Oceanics) was used to evaluate the volume of seawater filtered through the net. After sampling, the net was thoroughly externally rinsed with *in situ* seawater to concentrate debris in the collector screwed at the end of the net. The sample contained in the collector was then transferred into a hermetic glass jar. All samples were stored at −20 °C until treatment and analysis in the laboratory. Wind speed conditions encountered during seawater sampling are detailed for each study site in Table S1.

### 2.3. Pearl oyster sampling

In Ahe and Takaroa, a total of 14 pearl oysters were sampled across two livestock rearing areas of two pearl-farmers (7 individuals per farm). In Manihi, 14 oysters were supplied by only one pearl-farm (Fig. 1). Biometric measurement was realized before the dissection: mean oysters' height was 10.0 ± 1.7 cm (Ahe), 10.0 ± 1.1 cm (Manihi) and 9.8 ± 4.5 cm (Takaroa). The whole oyster flesh was then collected and individually packaged in zip-lock bags. Note that FTIR analysis was performed on a piece of zip-lock bag as negative control to ensure that no contamination was found in the oyster flesh. All samples were stored at −20 °C until treatment and analysis in the laboratory.

### 2.4. Sample treatment and analysis

#### 2.4.1. Particle isolation and quantification

Samples were processed in laboratory conditions under an extractor hood. Water samples were first cleaned of their macro-sized organic matter (*e.g.* leaves, seeds, macroalgae, fry) on sieves with a mesh size smaller than that of the nets used, *i.e.* 150 μm for the surface water samples and 30 μm for the water column samples. Macro-debris were rinsed with 1.2 μm-filtered distilled water before being removed to facilitate the digestion step. The digestion of organic matter was performed on the largest retained fraction following sieving (*i.e.* > 150 μm and > 30 μm) and according to the protocol of Dehaut et al. (2016), adapted by Foekema et al. (2013). Water samples were re-suspended in a 10% potassium hydroxide (KOH) solution in their respective hermetic glass jar with a stir bar and placed on a heating magnetic stirrer at 60 °C and 300 rpm for 24 h. The whole oyster flesh was thoroughly rinsed with 1.2 μm-filtered distilled water and placed in individual hermetic glass jar wherein it underwent the same digestion process in 100 ml of 10% KOH solution. After the first digestion step, samples were, once again, sieved on a 150 μm (surface water samples), 30 μm (water column samples), or 20 μm (pearl oyster samples) mesh sieve and thoroughly rinsed with filtered distilled water before re-suspension in a 30% hydrogen peroxide ($H_2O_2$) solution. The second digestion was performed at 50 °C and 300 rpm for 2 h before filtration on a GF/C filter (1.2 μm porosity, Ø 47 mm, Whatman®) previously burned at 450 °C. The filter was rinsed with filtered distilled water, then placed in a Petri dish for drying at room temperature before particle quantification. Filters were scanned using a high-resolution scanner (Epson Perfection 4990 PHOTO) at 12,800 dpi for numerical particle quantification with ImageJ software v.1.52. Scanner surface was carefully inspected and cleaned with filtered (1.2 μm) 70% ethanol. All of the particles (organic and inorganic), identified on the high-resolution scan of the filter, were pointed out, one by one, and quantified by dissociating fragments from fibres.

#### 2.4.2. Size distribution

Particle size analysis was performed with ImageJ software v1.52, using high-resolution scans of the filters. We focused on the cleaner filters (n = 4 per study site) for the samples for which the digestion step of organic matter had been the most efficient (*i.e.* no visible organic traces). Particle size was measured by setting a scale based on a known

distance in millimetres, converted into pixels. Contrast and threshold were adjusted in order to get as close as possible to the original picture. Particles were then fully analysed to obtain the width and the height of each in millimetres (mm). Width and height data were merged and classified according five size classes: 0.020–0.200, 0.200–0.335, 0.335–1, 1–5 and > 5 mm. Filters were analysed individually, then collected data were pooled from all study sites and treated separately according to sample type (*i.e.* surface water, water column and pearl oyster).

#### 2.4.3. Particle characterisation by Fourier transform-infrared (FTIR) spectroscopy

A subset of particles was randomly collected without *a priori* based on the work and procedures published by Kedzierski et al. (2019) (see Section 2.6) with ultra-precision tweezers used under microscope for subsequent FTIR analysis. FTIR microscopy measurements were then performed with a Thermo IS50 infrared spectrometer coupled to an infrared Thermo Nicolet™ Continuum™ microscope with a 15 × IR objective and a mercury cadmium telluride (MCT) single element detector cooled with liquid nitrogen. FTIR spectra were recorded at room temperature in the midIR range (400–4000 $cm^{-1}$). Each spectrum was averaged over 64 scans with a resolution of 4 $cm^{-1}$. A background scan was recorded prior measurement and subtracted from the sample spectra. In this method, colour of selected particles was monitored and single particles were then placed in a diamond micro-compression cell, one by one, and flattened between the two diamond anvils of a SPECAC® micro compression cell (Eurolabo, Paris, France). To obtain reliable results, comparison with a reference spectra database is absolutely necessary to unambiguously identify polymer type. Polymer identification was, therefore, made using the Thermo IR polymer database, with a 75% accuracy. Identified polymer types were categorized in three main groups: plastic, non-plastic and non-identifiable. The rayon polymer, which is often included in the classification of MP found in the marine environment, was excluded from this study. Indeed, FTIR-based studies showed that 30% of suspected rayon fibres turned out to be cellulose, which is a natural product. Since cellulose and the semi-synthetic polymer rayon have almost identical FTIR spectra (Lusher et al., 2014), we left this particular compound out of our study (Peeken et al., 2018).

#### 2.4.4. Multivariate analysis

To confirm the nature of the processed particles and analyse all spectra, we used chemometrics. The first step of this approach is to apply a spectral data pre-processing (Whittaker baseline correction) followed by a normalization method so that all the spectra would be at the same intensity, which facilitates the comparison with the database. The second step is to extract the meaningful information to identify the sample. Spectra were analysed using independent component analysis (ICA). ICA is a statistical and computational technique for extracting source signals from mixtures. The observed signals are considered as weighted sums of pure source signals, the weights being proportional to the contribution of the corresponding pure signals to each mixture (Hyvärinen and Oja, 2000; Wang et al., 2008). The objective of ICA is, therefore, to search for the least Gaussian possible sources, *i.e.* the most independent (Rutledge and Jouan-Rimbaud Bouveresse, 2013). Data treatment was done using MATLAB R2017a (The Math Works, Natick, USA).

Once polymer types were confirmed, microplastic concentrations were calculated by transposing the percentage of particles certified as plastic, in the sub-sampling of particles analysed by FTIR, to the total number of quantified particles for each sample (Kedzierski et al., 2019).

### 2.5. Quality control: contamination assessment and prevention

To reduce contamination from airborne particles, glass and stainless-steel material were used and all equipment were thoroughly rinsed with distilled water and 70% ethanol before use and/or immediately covered for preservation. All solutions (*i.e.* distilled water, ethanol, KOH, $H_2O_2$) were filtered through 1.2 µm glass microfibres filters (GF/C, Whatman®). After sampling, samples were quickly placed in hermetic glass jars to reduce air pollution. To minimize contamination within the laboratory, operators wore cotton lab coats at all times and frequently washed their hands. All surfaces were cleaned with filtered 70% ethanol and samples were always handled in a laminar flow hood.

To account for possible contaminations in the sample preparation process, background contamination from airborne particles during sampling was assessed by conducting field quality controls. To create this control for both surface water and water column sampling, an empty glass jar was left open on the vessel during sampling. Three quality controls were performed *in situ* for each study site (n = 9). Similar procedural blanks were also run in the lab (n = 27) at all steps of sample processing by leaving open an empty glass jar inside the hood whenever glass jars containing samples were open. An empty Petri dish with a clean filter was also established during FTIR analysis. Each field quality control and procedural blank jar was then rinsed with filtered distilled water that was filtered on a GF/C filter for particle quantification and characterization by FTIR. No FTIR analysis was performed on lab samples when the total of quantified particles was ≤ 10, considered as negligible (Pivokonsky et al., 2018; Wang et al., 2020).

### 2.6. Statistical approach and analyses

We used the statistical analysis proposed by Kedzierski et al. (2019) to define the sub-sampling procedure for conducting a representative analysis of our samples by determining "how many particles must be analysed to give a representative view of the particle size distribution and chemical nature, and calculate the associated margin error" (Kedzierski et al., 2019). Here, we decided to set the associated margin error at 15% (ε) considering the large total number of particles in samples of the three studied areas. In our configuration, in which the aim was to randomly sub-sample a specific number of particles (*n*), the total number of particles (*N*) was known. To this end, the following equation was used:

$$n = \frac{\frac{1}{4} + \frac{\varepsilon^2}{\left(u_{1-\frac{\alpha}{2}}\right)^2}}{\frac{\varepsilon^2}{\left(u_{1-\frac{\alpha}{2}}\right)^2} + \frac{1}{4N}}$$

where $u_{1-\frac{\alpha}{2}}$ is the fractal of order α of the standardized normal law. It is common to use a 95% degree of confidence (*i.e.* $\alpha = 0.05$; $u_{1-\frac{\alpha}{2}} = 1.96$) (Kedzierski et al., 2019).

All data were expressed as percentages (mean ± standard deviation, SD). Maps were produced based on mapping data from Andréfouët et al. (2006) and using QGIS software (v2.18.24).

## 3. Results

### 3.1. Background contamination

Microplastics were found in almost all control samples, with a median value of 7.2 (min = 0, max = 56.3; n = 9) and 8.8 (min = 0, max = 23.3; n = 15) MP/filter from *in situ* and lab samples, respectively. The particle size class distribution in the *in situ* samples was as follows: 0.020–0.200 mm (85.6 ± 5.6%), 0.200–0.335 mm (9.7 ± 4.1%), 0.335–1 mm (4.2 ± 2.2%), 1–5 mm (0.5 ± 1.2%), and > 5 mm (0%), while 100% of particles in the lab samples were in the 0.020–0.200 mm size class. The dominant shape in both *in situ* and lab controls was "fragment", with a median value of 4 (min = 0, max = 12; n = 9) and 5 (min = 0, max = 11; n = 15) item/filter, respectively, followed by "fibre" reaching a median value of 0 (min = 0, max = 2; n = 9) and 1 (min = 0,

max = 5; n = 15) item/filter, respectively. Detailed results on the background contamination from *in situ* and lab controls are presented in Tables S3 and S4, respectively. Nevertheless, background contamination was considered negligible since the number of MP in procedural blanks was < 5% of the total abundance of MP detected in corresponding samples (Pivokonsky et al., 2018; Wang et al., 2020) except for one sample from the lab, which reached 5.4% and corresponded to the digestion step of two pearl oysters from Takaroa. These two samples were removed prior to the analysis of MP concentration.

### 3.2. Particle characterization in marine compartments

#### 3.2.1. Surface water

*Total particles.* A total of 16,578 particles was quantified from the 33-manta trawl (335 μm-mesh) transects performed in the lagoons of Ahe, Manihi and Takaroa, representing a total volume of 5021 $m^3$ filtered seawater. Proportions of fragments and fibres (nature non-identified at this step) ranged from 83% to 86% and 14–17%, respectively, according to study site. The particle size class distribution was as follows: 0.020–0.200 mm (70.3 ± 14.5%), 0.200–0.335 mm (12.4 ± 5.3%), 0.335–1 mm (14.4 ± 9.0%), 1–5 mm (2.4 ± 1.1%), and > 5 mm (0.2 ± 0.4%) (Fig. 2 A). Please consider that the relative abundance of the 0.020–0.200 mm size class was expected to be underestimated because the net cannot capture all the particles smaller than its mesh size (335 μm).

*Microplastics.* Based on the statistical sub-sampling procedure (Kedzierski et al., 2019), 1571 particles were randomly selected for being characterized by FTIR spectroscopy. Synthetic matter was detected in all

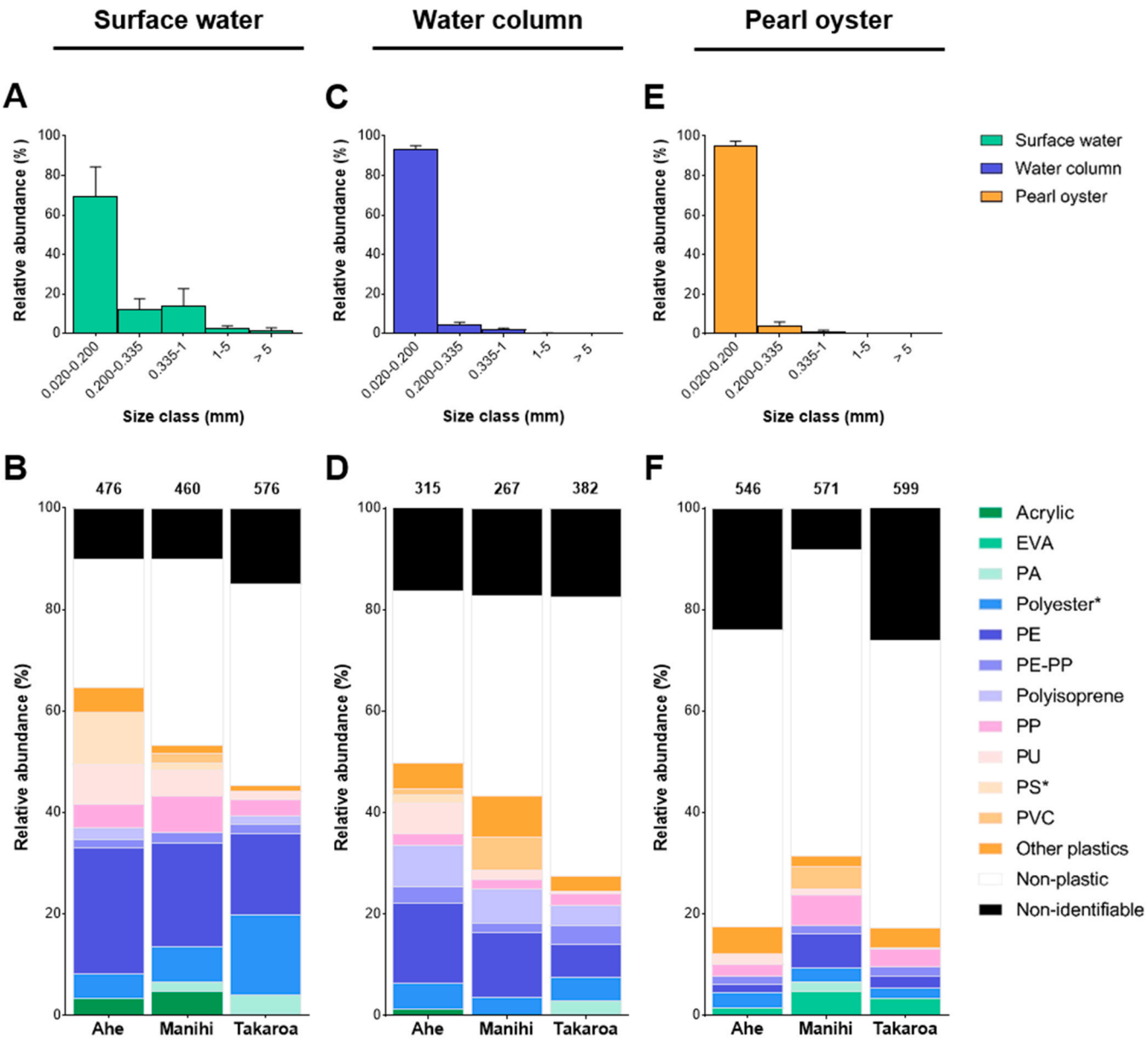


**Fig. 2.** Particle size class distribution (all sampling locations taken together) and microplastics distribution once identified by FTIR spectroscopy among study sites in surface water (A, B), water column (C, D) and pearl oyster (E, F). Particle size class distribution according to sample type (A, C and E) in samples from Ahe, Manihi and Takaroa (mean ± SD). Results of the FTIR analysis (B, D and F) illustrate the relative abundance of synthetic and natural ("non-plastic") matter as well as non-identifiable particles. Synthetic polymers commonly present in samples at > 1% are illustrated on the bar chart. Uncommon polymers and/or those < 1% are grouped under "other plastics". EVA: ethylene-vinyl acetate; PA: polyamide; Polyester (*including polyethylene terephthalate, PET); PE: polyethylene; PP: polypropylene; PS: polystyrene (*mostly styrene copolymer based), PU: polyurethane, PVC: polyvinyl chloride. Numbers at the top of each column of the histogram indicate the corresponding number of analysed particles (excluding the polymer rayon) based on the sub-sampling methodology of Kedzierski et al. (2019).

samples, composing 65%, 53% and 45% of analysed particles (classified as fragments or fibres) in Ahe, Manihi and Takaroa, respectively (Fig. 2B). Natural matter (*e.g.* cellulose, cotton or protein) was also detected in every sample, composing 25%, 37% and 40% of analysed particles in Ahe, Manihi and Takaroa, respectively (Fig. 2B). The remaining portion, *i.e.* 10%, 10% and 15% in Ahe, Manihi and Takaroa, respectively, was assigned to non-identifiable particles (*i.e.* particles whose spectra did not match any of those present in the databases, so that no signal was obtained). Corresponding raw data of particles analysed by FTIR and their relative abundance in surface water samples are given in Table S5. Totals of 308, 245 and 270 particles were certified as microplastics for Ahe, Manihi and Takaroa, respectively. The three most abundant synthetic polymers among MP according to study sites were as follows: Ahe, polyethylene (PE) = 38.6% (n = 119); polyurethane (PU) = 15.6% (n = 48); polystyrene (PS) = 12.3% (n = 38); Manihi, PE = 38.0% (n = 93); polypropylene (PP) = 13.5% (n = 33); polyester = 13.5% (n = 33); and Takaroa, polyester = 34.1% (n = 92); PE = 33.7% (n = 91); polyamide (PA) = 8.5% (n = 23). Note that the relative abundance of polyester includes polyethylene terephthalate (PET). They are the same polymer but named differently according to the use (*e.g.* polyester in fibres, PET in food packaging). The relative abundance of synthetic polymers certified in surface water samples according to study sites are detailed in Table S6.

Microplastics from surface water were dominated by particles of a black/grey colour (39.8 ± 14.4%) followed by blue (15.0 ± 2.8%) and red (12.6 ± 10.4%) MP (Fig. 3A). Black/grey MP were most frequently PE (44.3 ± 2.8%), PP (14.4 ± 7.7%) (Fig. 4), PS (8.1 ± 1.2%) and PE-PP (7.5 ± 1.3%). Blue MP were represented by PE (41.7 ± 10.4%), polyester (19.5 ± 2.3%) and acrylic (14.8 ± 9.7%) and red MP were predominantly polyester (45.2 ± 29.8%) and PE (17.2 ± 23.9%). Raw data on MP colour distribution and corresponding polymer types predominance are detailed in Table S7.

To test the potential implication of pearl-farming in the generation of black/grey PE and PP MP mostly found (Fig. 4C-D), samples of visually black/grey ropes (Fig. 4E) and spat collectors (Fig. 4E) were collected in the field and examined by FTIR. The FTIR results identified PE, PP, and copolymer PE-PP for both these types of pearl-farming gear (Fig. 4A-B).

### 3.2.2. Water column

*Total particles.* A total of 18,427 particles was counted from the 27 vertical samplings with the planktonic net (40 μm-mesh) performed in the lagoons of Ahe (depth of 14–54 m), Manihi (depth of 27–46 m) and Takaroa (depth of 8–45 m), representing volumes of filtered seawater ranging from 0.8 to 5.1 $m^3$. Proportions of fragments and fibres ranged from 88% to 92% and 8–12%, respectively, according to study site. The particle size class distribution was as follows: particles 0.020–0.200 mm (93.2 ± 1.8%), 0.200–0.335 mm (4.4 ± 1.4%), 0.335–1 mm (2.1 ± 0.7%), 1–5 mm (0.3 ± 0.16%) and no particles were found in the > 5 mm size class (Fig. 2 C). Please consider that the relative abundance of the 0.020–0.200 mm size class was expected to be underestimated because the net cannot capture all the particles smaller than its mesh size (40 μm).

*Microplastics.* A total of 991 particles was randomly selected among study sites and characterized. FTIR identification revealed the presence of synthetic matter in 50%, 43% and 27% of particles in Ahe, Manihi and Takaroa, respectively (Fig. 2D). Natural matter was marked by the presence of mineral compounds, especially in Takaroa atoll where it represented 16% of particles (Table S8). Relative abundance associated with natural matter reached 34%, 39% and 55% of particles in samples from Ahe, Manihi and Takaroa, respectively (Fig. 2D). Non-identifiable particles accounted for 16–17% according to study site. Corresponding raw data of analysed particles and their relative abundance in water column samples are given in Table S8. Totals of 157, 108 and 103 microplastic particles were certified for Ahe, Manihi and Takaroa, respectively. The three most abundant synthetic polymers among MP according to study sites were as follows: Ahe, PE = 31.8% (n = 50); polyisoprene = 16.6% (n = 26); PS = 12.1% (n = 19); Manihi, PE = 31.5% (n = 34); polyisoprene = 16.7% (n = 18); polyvinyl chloride (PVC) = 15.7% (n = 17); and Takaroa, PE = 24.3% (n = 25); polyester = 17.5% (n = 18); polyisoprene = 14.6% (n = 15). The relative abundance of synthetic polymers certified in water column samples according to study sites is detailed in Table S9.

Microplastics from the water column were dominated by particles of a black/grey colour (45.4 ± 4.7%) followed by orange (14.4 ± 1.4%) and yellow (12.6 ± 7.6%) MP (Fig. 3B). Black/grey MP were most frequently PE (39.5 ± 10.6%), PE-PP (15.1 ± 11.0%) and PP (11.7 ± 7.0%) (Fig. 4). Orange MP were dominated by polyisoprene (81.7 ± 6.4%) and yellow MP included PS (19.6 ± 29.3%), PVC (24.1 ± 41.7%, mostly from Manihi) and polyisoprene (24.1 ± 23.1%). Raw data on MP colour distribution and the corresponding predominance of the different polymer types are detailed in Table S7.

### 3.2.3. Pearl oyster

*Total particles.* A total of 11,083 particles was found in the digesta of 42 pearl oysters from the three lagoons. Proportions of fragments and fibres ranged from 70% to 96% and 4–30%, respectively, according to study site. The particle size class distribution was as follows: particles 0.020–0.200 mm (95.0 ± 2.3%), 0.200–0.335 mm (4.1 ± 1.9%), 0.335–1 mm (0.9 ± 0.9%), and no particles were found in the 1–5 mm or > 5 mm size classes (Fig. 2E).

*Microplastics.* A total of 1908 particles from pearl oyster samples were identified by FTIR spectroscopy. Composition of particles was

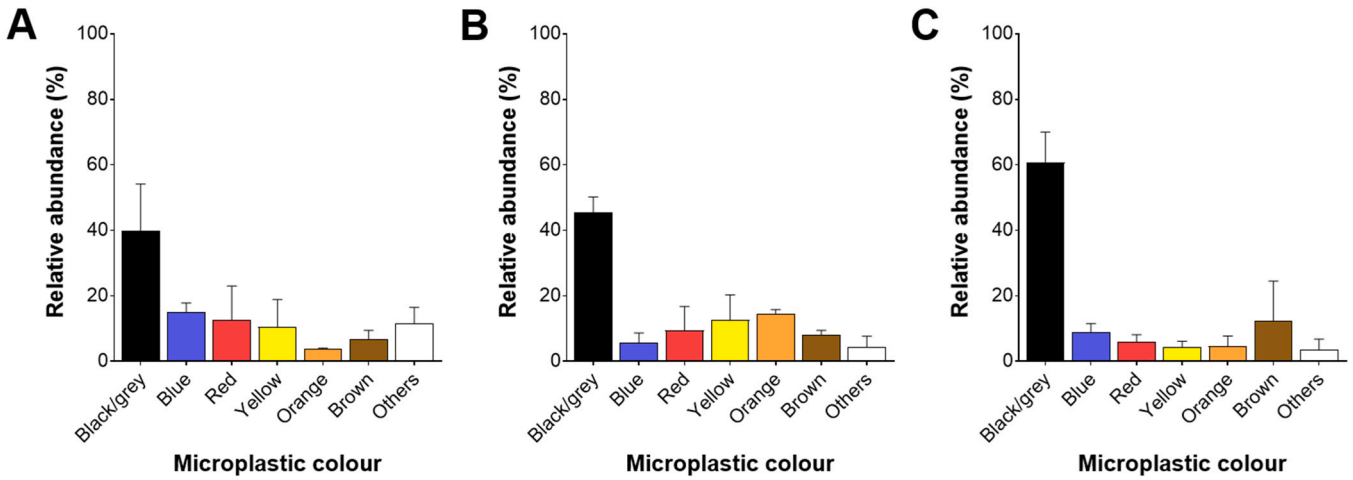


**Fig. 3.** Microplastic colour distribution in surface water (A), water column (B) and pearl oyster (C) samples, all study sites taken together.

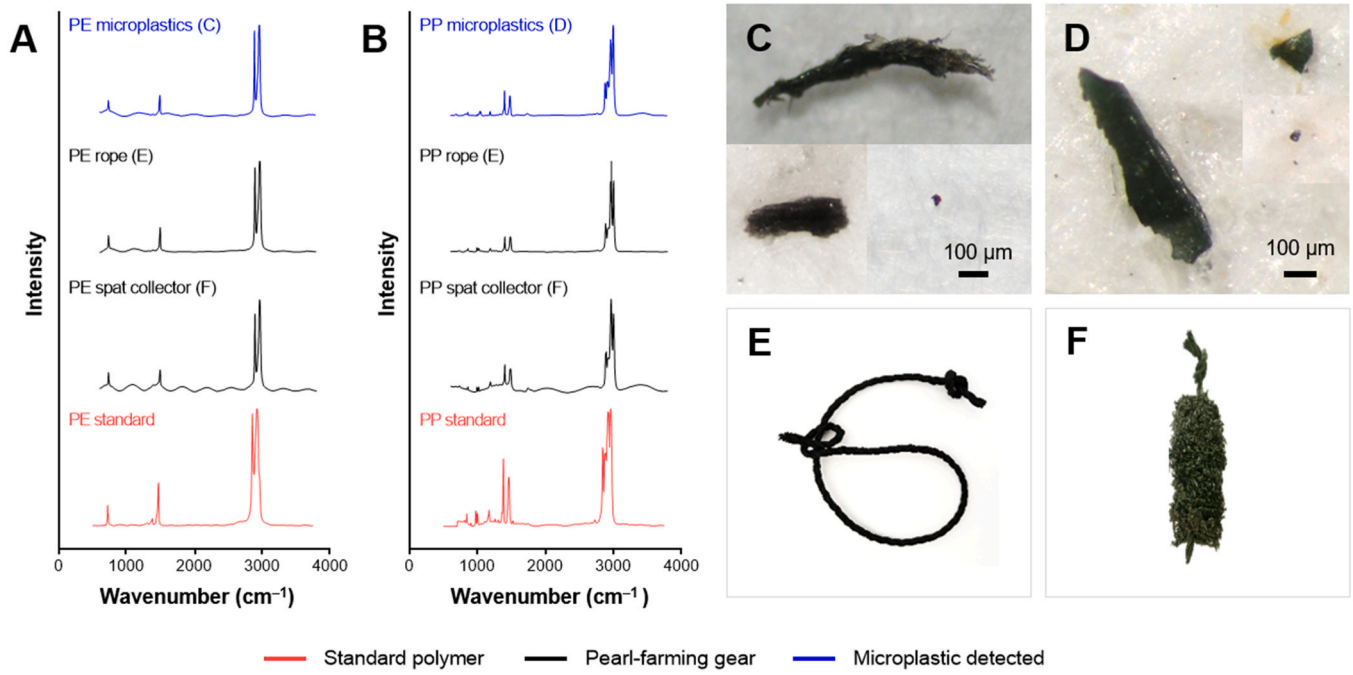


**Fig. 4.** FTIR spectra of the black/grey microplastics mostly detected in both surface water and water column and the pearl-farming gears, visually black/grey, collected from pearl-farming lagoons. Spectral comparisons between PE (A) and PP (B) microplastic samples and their possible sources of origin associated with rope and spat collector, both identified as PE, PP or copolymer PE-PP. Illustrations of PE microplastics (C), PP microplastics (D), rope (E) and spat collector (F).

dominated by natural matter representing 59%, 60% and 57% of particles, whereas synthetic matter represented 17%, 31% and 17% of particles in samples from Ahe, Manihi and Takaroa, respectively (Fig. 2F). Natural matter was marked by the presence of residual organic matter such as pigments (3–11%) and proteins (3–7%) (Table S10). Non-identifiable particles ranged from 8% to 26% according to study site (Fig. 2F). Raw data associated with composition and abundance of particles identified in pearl oyster samples are detailed in Table S10. Totals of 90, 178 and 104 microplastic particles were certified for Ahe, Manihi and Takaroa, respectively. The three most abundant synthetic polymers among MP according to study sites were as follows: Ahe, polyester = 18.9% (n = 17); PP = 14.4% (n = 13); PS = 12.2% (n = 11); Manihi, PE = 21.3% (n = 38); PP = 19.7% (n = 35); ethylene-vinyl acetate (EVA) = 15.2% (n = 27); and Takaroa, PP = 20.2% (n = 21); EVA = 19.2% (n = 20); PE = 14.4% (n = 15). The relative abundance of synthetic polymers certified in pearl oyster samples according to study sites is detailed in Table S11.

Microplastics in the pearl oyster samples were dominated by black/grey colours (60.7 ± 9.3%) followed by brown (12.2 ± 12.3%) and blue (8.8 ± 2.8%) MP (Fig. 3C). Black/grey MP were mostly PP (25.0 ± 8.0%), EVA (20.1 ± 9.1%), PE (13.4 ± 0.6%) and PE-PP (9.8 ± 3.8%). Brown MP included particles of PVC (25.0 ± 25.0%, mostly from Manihi), PE (30.9 ± 27.0%), PE-PP (13.3 ± 21.0%) and blue MP were dominated by polyester (32.2 ± 11.3%), PS (17.0 ± 20.6%) and EVA (14.4 ± 6.8%). Raw data of MP colour distribution and corresponding polymer type predominance are detailed in Table S7.

### 3.3. Microplastics concentration and distribution

In Ahe, MP concentrations ranged from 0.5 to 8.3 item $m^{-3}$ in surface water, from 22.1 to 217.2 item $m^{-3}$ in water column and from 2.6 to 41.9 item $g^{-1}$ standardized (std) dry weight (dw) in pearl oyster. MP concentrations were relatively homogeneous in surface water whatever the sampling stations with a slight tendency to be higher in the centre part of the lagoon adjacent to the pass, where concentrations were three times higher in inflow than in outflow sea currents (Fig. 5A). Otherwise, a particular pattern was observed considering MP distribution in the water column, showing higher concentrations in the south of the atoll, at stations 1, 2 and 4 (Fig. 5A). Spatial distribution and concentrations of MP from Ahe are illustrated in Fig. 5A and detailed in Table S2.

In Manihi, MP concentrations ranged from 1.0 to 8.4 item $m^{-3}$ in surface water, from 27.8 to 130.2 item $m^{-3}$ in water column and from 5.7 to 125.0 item $g^{-1}$ std dw in pearl oyster. Similar patterns of MP distribution than Ahe atoll were observed in both surface water and water column, with higher concentrations recorded in the centre and northern parts of the atoll lagoon (stations 4, 5, 6, 7, 8 and 9), while similar values were observed in the pass regardless of the direction of the current (Fig. 5B). Spatial distribution and concentrations of MP from Manihi are illustrated in Fig. 5B and detailed in Table S2.

In Takaroa, MP concentrations ranged from 0.2 to 3.2 item $m^{-3}$ in surface water, from 22.7 to 716.2 item $m^{-3}$ in water column and from 2.1 to 54.2 item $g^{-1}$ std dw in pearl oyster. MP concentrations were relatively homogeneous in surface water for all the sampling stations except station 3, directly opposite the pass, where the highest concentration was measured although similar values were observed in the pass regardless of the current direction (Fig. 5C). Otherwise, a particular pattern of MP distribution in water column was observed, with higher concentrations in the southern part of the atoll lagoon (station 1, 2 and 3; Fig. 5C). Spatial distribution and concentrations of MP from Takaroa are illustrated in Fig. 5C and detailed in Table S2.

The average MP concentrations (mean ± SD) recorded in surface water, water column and cultivated pearl oysters according to the three study sites are illustrated in Fig. 5. Main characteristics of the microplastics contamination in pearl-farming lagoons of French Polynesia are summarized in Table 1.

## 4. Discussion

### 4.1. Widespread contamination of pearl-farming lagoons by microplastics

Microplastics were detected in all compartments investigated: surface water, water column and cultivated pearl oysters. Focusing on surface water contamination, monitored according to a method

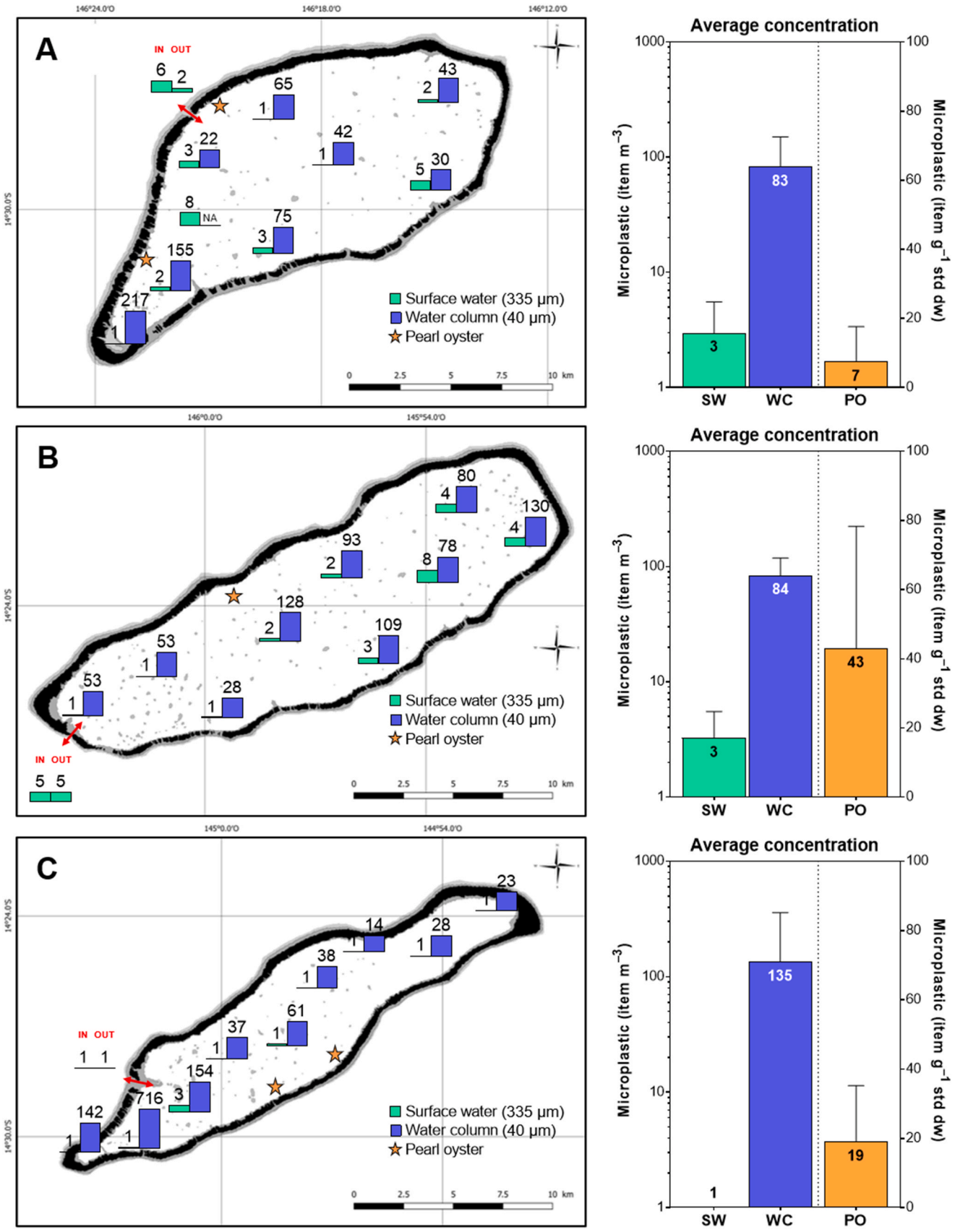


**Fig. 5.** Spatial distribution and concentration (item $m^{-3}$ or item $g^{-1}$ standardized dry weight for pearl oysters) of microplastics in Ahe (A), Manihi (B) and Takaroa (C). SW: surface water; WC: water column; PO: pearl oyster.

**Table 1**
Summary of main characteristics of the microplastics contamination in pearl-farming lagoons of French Polynesia.

| | Study site | | |
|---|---|---|---|
| | **Ahe** | **Manihi** | **Takaroa** |
| **Microplastic characteristics** | | | |
| *Dominant shape* | | | |
| SW | Fragment (86%) | Fragment (83%) | Fragment (83%) |
| WC | Fragment (91%) | Fragment (92%) | Fragment (88%) |
| PO | Fragment (70%) | Fragment (96%) | Fragment (87%) |
| *Dominant colour* | | | |
| SW | Black/grey (30%) | Black/grey (56%) | Black/grey (33%) |
| WC | Black/grey (40%) | Black/grey (50%) | Black/grey (46%) |
| PO | Black/grey (66%) | Black/grey (50%) | Black/grey (66%) |
| *Dominant polymer type* | | | |
| SW | Polyethylene (39%) | Polyethylene (38%) | Polyethylene (34%) |
| WC | Polyethylene (32%) | Polyethylene (32%) | Polyethylene (24%) |
| PO | Polyester (19%) | Polyethylene (21%) | Polypropylene (20%) |
| *Dominant size class (μm)* | | | |
| SW[a] | 20–200 (74%) | 20–200 (57%) | 20–200 (80%) |
| WC[a] | 20–200 (93%) | 20–200 (93%) | 20–200 (95%) |
| PO | 20–200 (95%) | 20–200 (95%) | 20–200 (96%) |
| **Microplastic concentrations (mean ± SD)** | | | |
| SW (MP $m^{-3}$) | 3.0 ± 2.6 | 3.3 ± 2.3 | 0.9 ± 0.9 |
| WC (MP $m^{-3}$) | 82.6 ± 67.6 | 83.6 ± 35.1 | 134.7 ± 224.0 |
| PO (MP $g^{-1}$ std dw / MP individual$^{-1}$) | 7.5 ± 10.1 / 23.0 ± 20.7 | 43.0 ± 35.3 / 137.6 ± 89.4 | 19.1 ± 16.1 / 39.5 ± 42.6 |

SW: surface water (335 μm-mesh); WC: water column (40 μm-mesh); PO: pearl oyster (> 20 μm).
[a] Values that are expected to be underestimated since smaller microplastics (but certainly not all) than net-mesh sizes, used to monitor both SW (335 μm) and WC (40 μm), were caught.

commonly used and recommended worldwide (*i.e.* a manta trawl with a 335 μm-mesh; Hidalgo-Ruz et al., 2012), the mean MP concentration found in Polynesian pearl-farming atolls (2.4 ± 2.3 MP $m^{-3}$) was higher than those found in other coastal ecosystems such as the Bay of Brest in France (0.2 ± 0.3 MP $m^{-3}$) (Frère et al., 2017), Bohai Sea in China (0.3 ± 0.3 MP $m^{-3}$) (Zhang et al., 2017) or the semi-enclosed north-western Mediterranean Sea (ranging from 0.1 to 0.3 MP $m^{-3}$) (de Lucia et al., 2014), even though these other areas are under greater demographic pressure than the atolls in our study (which have 491–674 inhabitants). The MP concentrations recorded in Ahe and Manihi are similar to recordings from sites already analysed on the Hong Kong coast in China (4.0 ± 1.2 MP $m^{-3}$) (Cheung et al., 2018) and East Asian Seas (3.7 ± 10.4 MP $m^{-3}$) (Isobe et al., 2015). Furthermore, an underestimation of surface water MP concentration was suspected at Takaroa due to a strong north-easterly wind regime (~ 10 knots) throughout the sampling period, which likely disturbed the vertical repartition of MP in the upper layers of the water column (Collignon et al., 2012). As a global trend, Poulain et al. (2019) estimated that corrected microplastic concentrations were 2.4–5006 times more abundant than uncorrected ones, the highest difference being obtained for large MP (1–5 mm) using the ellipsoid model. By correcting the concentrations of MP floating at the sea surface in Takaroa lagoon using the modelling approach introduced by Kukulka et al. (2012) (Table S2), the obtained corrected concentrations calculated were indeed higher than uncorrected ones reaching an order of magnitude of $10^3$ to $10^4$ which appeared surprisingly high whereas the wind reached 5.5 m $s^{-1}$ during the sampling campaign, meaning 0.5 m $s^{-1}$ above the limit considered negligible. They must therefore be considered with caution to avoid overestimating the concentration of floating MP. The high variability in MP levels observed at the sea surface of Takaroa may also be driven by the presence of accumulation areas created by waves, winds (Kim et al., 2015; Kukulka et al., 2016; Liubartseva et al., 2016) and hydrodynamic factors (Rocha-Santos and Duarte, 2015) that are mainly determined by the current flow through the pass in such lagoons. For instance, the highest concentrations of floating MP recorded in Ahe and Takaroa were in the southern areas that are considered as accumulation areas (*i.e.* showing many suspended particles and high turbidity), less subject to water renewal from the current flow of the pass and strengthened by the influence of the dominant wind (NE, ENE). The occurrence of such MP accumulation zones protected from pass inflow and outflow is also supported by a hydrodynamic model made in Ahe and coincides with pearl oyster larval trajectories (Thomas et al., 2016). An opposite pattern was observed in Manihi since the pass is located in the south of the atoll leading to an accumulation area in the northern part, which is less subjected to water renewal. Although Manihi is the largest studied atoll (165 $km^2$) with the lowest number of authorized concessions (*i.e.* n = 498), it displayed the highest concentration of floating MP and pearl oyster contamination levels. This result could, therefore, be linked to lower water renewal, which reaches 130 days of residence time, in contrast to 34 and 76 days of residence time in Ahe and Takaroa, respectively (Pagès et al., 2001). Overall, these results suggest that these remote insular territories are subjected to significant MP contamination pollution and that water currents going in and out through the passes may strongly influence floating debris concentration, distribution and accumulation in the lagoons.

### 4.2. *The water column is a highly contaminated compartment in French Polynesia lagoons*

Monitoring MP in the water column in addition to surface water enabled us to draw a more complete picture of lagoon contamination and to estimate the exposition levels of cultivated pearl oysters reared in the water column (4–6 m depth).

The comparison between surface water and water column contamination is poorly relevant in our study since these two compartments were investigated with two different sampling methodologies (manta trawl with a 335 μm-mesh *vs.* planktonic net with a 40 μm-mesh). Indeed, recent studies highlighted that reported microplastic concentrations diverged depending on different sampling strategies and decreased exponentially with greater mesh size (Green et al., 2018; Covernton et al., 2019; Lindeque et al., 2020). For example, Lindeque et al. (2020) demonstrated that microplastic concentration using a 100 μm net was 10-fold greater than a 500 μm net. Therefore, the MP abundance in the water column (8–54 m depth), almost two orders of magnitude higher (range 6–594) than that in surface water in our study, remains speculative and we cannot draw conclusions about the most

contaminated compartment. Nonetheless, we demonstrated that the water column of study sites is a highly contaminated compartment that is of further interest to monitor through a spatio-temporal series. Significant quantities of MP have also been detected in water bodies of the Bohai Sea (5–30 m depth; Dai et al., 2018), in Korean coastal waters (3–58 m depth; Song et al., 2018) and in the Arctic Ocean (6 m depth; Lusher et al., 2015), suggesting that levels in this compartment may be largely underestimated. The high proportion of MP sequestered in the water column is caused by vertical movement of which the rising and sinking velocities depend on polymer density, size and shape (Enders et al., 2015; Ballent et al., 2016). In our study, PE and polyisoprene were the predominant polymer types in the water column despite their low density (0.917–0.965 g $cm^{-3}$; Hidalgo-Ruz et al., 2012). Previous studies have provided evidence of the influence of wind, surface heat fluxes and Langmuir turbulence on vertical mixing of buoyant MP and MP concentrations in surface water (Kukulka et al., 2012, 2016). Biological processes such as biofouling (Fazey and Ryan, 2016), aggregation (Bergmann et al., 2017) or ingestion-egestion by marine organisms (Cole et al., 2016), may also have an effect on MP buoyancy (Kooi et al., 2017). Both observational and modelling studies have also shown that small MP have shorter residence times in the surface layer (Eriksen et al., 2014; Enders et al., 2015). Studies dealing with vertical profiles of MP distribution are very scarce and the lack of standardized protocols hampers thorough comparison of results from different compartments. For instance, studies have employed non-similar sampling tools, mesh sizes, sampling depths or laboratory sample processing protocols, making quantitative comparison difficult (Hidalgo-Ruz et al., 2012). Overall, these results remind us of the knowledge gap regarding the vertical behaviour of MP at sea, and of how environmental surveys of surface waters are far from sufficient for evaluating concentrations and ecological risks related to MP in the water body.

### 4.3. Dominance of small-sized, fragment-shaped and polyethylene microplastics in seawater

The main size class of MP observed in seawater was 20–200 μm both in surface water and the water column even if this class might be considered as underestimated. Smaller MP were caught than the net-mesh size (but not all as below the mesh), particularly in surface water (> 335 μm), probably due to homo- and/or heteroaggregation (Zhao et al., 2017). In this study, fragments were identified as the dominant form of MP in seawater (ranging from 83% to 92%) throughout the three study sites. The dominance of fragments over fibres suggests that the source of MP in the monitored lagoons is more related to the breakdown of larger plastic debris (Andrady, 2011) than to direct primary inputs such as domestic waste from nearby villages, including sewage contaminated by fibres from washing clothes (Yuan et al., 2019). This pattern may result from Polynesian dressing habits, as tropical environment involves the use of less clothing that produces lots of fibres (*e.g.* synthetic knitwear or fleece; Napper and Thompson, 2016) as well as the relatively small human populations (491–674 inhabitants) residing on the studied atolls. Human activity at sea is also a source of plastic pollution, notably fishing and aquaculture (Lebreton et al., 2018). In case of intense mariculture activity, especially in a semi-enclosed narrow bay, mariculture-derived MP made up approximately 56% and 37% of the MP in the seawater and sediment of the Xiangshan Bay in China (Chen et al., 2018). Atoll lagoons are also semi-enclosed environments. Thus, considering (i) the high MP contamination levels in the lagoons, (ii) the low population density and (iii) the high proportion of secondary microplastics (plastic fragments) in all samples, it is likely that maritime activities, including pearl-farming, and their associated waste (already demonstrated at the macrowaste level; Andréfouët et al., 2014) could be a source of MP environmental pollution.

We identified 31 synthetic polymers, among which polyethylene (PE) was the dominant polymer type in surface water (34–39%) and the water column (24–32%), as found by most other studies (Frère et al., 2017; Zhu et al., 2018; Pan et al., 2019; Zhang et al., 2020) as a consequence of its worldwide manufacture and use (PlasticsEurope, 2020). PE was followed by polyester, polyamide (PA), polypropylene (PP), polyurethane (PU), and polystyrene (PS) in surface water, while polyisoprene and polyester were prevalent in the water column. According to a source-specific classification system reported by Wang et al. (2019) and an assessment of MP derived from mariculture in Xiangshan Bay, China (Chen et al., 2018), fishing ropes, lines and nets are most likely important sources of PE, PP, PE-PP and PA in the aquatic ecosystem. Here we suggested that synthetic ropes and spat collectors contribute significantly to the MP pollution. Indeed, synthetic ropes and spat collectors, the main plastic equipment used in pearl-farming, are made of PE or PP, respectively (though sometimes both may be made in PE-PP) and are black-grey like the most sampled MP represented by black-grey PE, PP and PE-PP. Overall, the assessment of MP pollution in atoll lagoons without any pearl-farming pressure would provide a relevant means of comparison to examine the influence of pearl-farming activity in MP contamination of lagoons.

### 4.4. Seawater contamination is reflected in cultivated pearl oysters

Size frequency distribution of all the particles analysed in pearl oyster samples corresponded to the particle size range retained by *P. margaritifera* when feeding (*i.e.* 2–200 μm; Pouvreau et al., 1999); the 20–200 μm fraction accounted for 95% of all particles. Our lower size threshold of detection for particles was 20 μm (limit imposed by visual observation and manual selection with ultra-precision tweezers). However, upper size ranges of 200–335 μm (4%) and 335–1000 μm (1%) were present although unexpected. Even if pearl oyster samples were rinsed before underwent the digestion process, it is possible that particles were trapped in the gills or on the outside of the oyster soft tissues rather than being present in the digestive tract. Indeed, adherence of MP to mussel soft tissue has been proposed as an additional uptake pathway for MP alongside ingestion (Kolandhasamy et al., 2018).

In this study, we identified MP in all pearl oysters collected in the study sites. This 100% presence is close to some observations made in wild mussels, *Mytilus galloprovincialis*, *Choromytilus meridionalis* and *Aulacomya ater* (98%, n = 168) sampled in southern Africa (Sparks, 2020) or cultivated mussels, *Mytilus edulis* (90%, n = 120) sampled on French coasts (Phuong et al., 2018). However, the mean MP concentrations ranging from 7.5 to 43.0 MP $g^{-1}$ dry weight (dw) in cultivated pearl oysters are much higher (1.3–7.3 MP $g^{-1}$ wet weight: ww; using a conversion factor from dw to ww of 6 assuming a lyophilization rate of 0.17) than those reported in *C. gigas* and *M. edulis* reared in the North Sea ($0.47 \pm 0.16$ and $0.36 \pm 0.07$ MP $g^{-1}$ ww, respectively; Van Cauwenberghe and Janssen, 2014) and in the range of those found in *M. edulis* from Chinese coastal waters (1.5–5.4 MP $g^{-1}$ ww; Qu et al., 2018). While studies have shown a higher MP contamination in cultivated mussels than wild ones (Mathalon and Hill, 2014; Phuong et al., 2018), supposedly due to a proximity of MP coming from degradation of the plastic materials (PE, PP, polyester) of collectors, ropes and nets used in bivalve aquaculture (Phuong et al., 2018), in our study, we did not evaluate MP contamination in wild pearl oysters since wild individuals are protected by a local law. The majority of MP found in pearl oyster is fragments, reaching 73–95% of all particles, made of PE, PP, PE-PP, polyester and ethylene-vinyl acetate (EVA). This pattern corresponds to water body contamination such as the positive relationship observed in the coastal waters of China between mussels and water contamination patterns (Qu et al., 2018). Our study showed that MP contamination was widespread in pearl oysters and that *P. margaritifera* could be used as an indicator of MP pollution in French Polynesian lagoons.

## 5. Conclusion

Our findings demonstrate the widespread MP contamination of

pearl-farming atoll lagoons, with the dominance of small-sized fragments (20–200 μm) in the water column as well as in pearl oysters. This raises the question of the potential threat posed by microplastics to cultivated pearl oysters and the overall balance of the lagoon ecosystem. Further work is needed to understand this emerging risk and to predict potential impacts on pearl oyster and pearl-farming sustainability. These *in situ* data will make it possible to test relevant environmental scenarios as accurately as possible (*i.e.* real concentrations and specific MP types) on *P. margaritifera* in laboratory conditions to obtain more pertinent answers to local policies. Finally, these first data call for larger spatio-temporal studies with reliable methodology for the different compartments and with a special focus on sources, the key to local decision support.

## CRediT authorship contribution statement

**Tony Gardon**: Conceptualization, Methodology, Validation, Formal analysis, Investigation, Resources, Writing - original draft, Writing - review & editing, Visualization, Supervision. **Maria El Rakwe**: Conceptualization, Software, Formal analysis, Investigation, Resources, Writing - original draft, Writing - review & editing, Visualization. **Ika Paul-Pont**: Conceptualization, Methodology, Validation, Writing - original draft, Writing - review & editing, Supervision. **Jérémy Le Luyer**: Validation, Writing - original draft, Writing - review & editing, Supervision. **Léna Thomas**: Formal analysis, Investigation, Resources. **Enora Prado**: Formal analysis, Investigation, Resources. **Kada Boukerma**: Formal analysis, Investigation, Resources. **Anne-Laure Cassone**: Formal analysis, Investigation, Resources. **Virgile Quillien**: Investigation, Resources. **Claude Soyez**: Investigation. **Louis Costes**: Formal analysis, Resources. **Margaux Crusot**: Formal analysis. **Catherine Dreanno**: Supervision. **Gilles Le Moullac**: Conceptualization, Methodology, Validation, Investigation, Resources, Writing - original draft, Supervision, Project administration, Funding acquisition. **Arnaud Huvet**: Conceptualization, Methodology, Validation, Investigation, Resources, Writing - original draft, Writing - review & editing, Supervision.

## Declaration of Competing Interest

The authors declare that they have no known competing financial interests or personal relationships that could have appeared to influence the work reported in this paper.

## Acknowledgements

This study was financially supported by the MICROLAG project funded by Direction des Ressources Marines (DRM) of French Polynesia. T. Gardon was funded by a Doctoral Research Grant No. 09793 from Institut français de recherche pour l'exploitation de la mer (Ifremer). We really thank M. Kedzierski for helpful assistance defining the subsampling procedure. Our thanks extend to boat drivers G. Haumani (DRM) and M. Matarere (Ifremer) as well as pearl-farmers who supplied us with pearl oysters.

## Appendix A. Supporting information

Supplementary data associated with this article can be found in the online version at doi:10.1016/j.jhazmat.2021.126396.

## References

Andrady, A.L., 2011. Microplastics in the marine environment. Mar. Pollut. Bull. 62, 1596–1605. https://doi.org/10.1016/j.marpolbul.2011.05.030.

Andréfouët, S., Muller-Karger, F.E., Robinson, J.A., Torres-Pulliza, D., Spraggins, S.A., Murch, B., 2006. Global assessment of modern coral reef extent and diversity for regional science and management applications: a view from space 14.

Andréfouët, S., Thomas, Y., Lo, C., 2014. Amount and type of derelict gear from the declining black pearl oyster aquaculture in Ahe atoll lagoon, French Polynesia. Mar. Pollut. Bull. 83, 224–230. https://doi.org/10.1016/j.marpolbul.2014.03.048.

Ballent, A., Corcoran, P.L., Madden, O., Helm, P.A., Longstaffe, F.J., 2016. Sources and sinks of microplastics in Canadian Lake Ontario nearshore, tributary and beach sediments. Mar. Pollut. Bull. 110, 383–395. https://doi.org/10.1016/j.marpolbul.2016.06.037.

Barnes, D.K.A., Galgani, F., Thompson, R.C., Barlaz, M., 2009. Accumulation and fragmentation of plastic debris in global environments. Philos. Trans. R. Soc. B Biol. Sci. 364, 1985–1998. https://doi.org/10.1098/rstb.2008.0205.

Bergmann, M., Wirzberger, V., Krumpen, T., Lorenz, C., Primpke, S., Tekman, M.B., Gerdts, G., 2017. High quantities of microplastic in arctic deep-sea sediments from the HAUSGARTEN observatory. Environ. Sci. Technol. 51, 11000–11010. https://doi.org/10.1021/acs.est.7b03331.

Boucher, J., Friot, D., 2017. Primary Microplastics in the Oceans. Boucher.

Chen, M., Jin, M., Tao, P., Wang, Z., Xie, W., Yu, X., Wang, K., 2018. Assessment of microplastics derived from mariculture in Xiangshan Bay, China. Environ. Pollut. 242, 1146–1156. https://doi.org/10.1016/j.envpol.2018.07.133.

Cheung, P.K., Fok, L., Hung, P.L., Cheung, L.T.O., 2018. Spatio-temporal comparison of neustonic microplastic density in Hong Kong waters under the influence of the Pearl River Estuary. Sci. Total Environ. 628–629, 731–739. https://doi.org/10.1016/j.scitotenv.2018.01.338.

Cole, M., Webb, H., Lindeque, P.K., Fileman, E.S., Halsband, C., Galloway, T.S., 2015. Isolation of microplastics in biota-rich seawater samples and marine organisms. Sci. Rep. 4. https://doi.org/10.1038/srep04528.

Cole, M., Lindeque, P.K., Fileman, E., Clark, J., Lewis, C., Halsband, C., Galloway, T.S., 2016. Microplastics alter the properties and sinking rates of zooplankton faecal pellets. Environ. Sci. Technol. 50, 3239–3246. https://doi.org/10.1021/acs.est.5b05905.

Collignon, A., Hecq, J.-H., Glagani, F., Voisin, P., Collard, F., Goffart, A., 2012. Neustonic microplastic and zooplankton in the North Western Mediterranean Sea. Mar. Pollut. Bull. 64, 861–864. https://doi.org/10.1016/j.marpolbul.2012.01.011.

Connors, E.J., 2017. Distribution and biological implications of plastic pollution on the fringing reef of Mo'orea, French Polynesia. PeerJ 5, 3733. https://doi.org/10.7717/peerj.3733.

Covernton, G.A., Pearce, C.M., Gurney-Smith, H.J., Chastain, S.G., Ross, P.S., Dower, J. F., Dudas, S.E., 2019. Size and shape matter: a preliminary analysis of microplastic sampling technique in seawater studies with implications for ecological risk assessment. Sci. Total Environ. 667, 124–132. https://doi.org/10.1016/j.scitotenv.2019.02.346.

Dai, Z., Zhang, H., Zhou, Q., Tian, Y., Chen, T., Tu, C., Fu, C., Luo, Y., 2018. Occurrence of microplastics in the water column and sediment in an inland sea affected by intensive anthropogenic activities. Environ. Pollut. 242, 1557–1565. https://doi.org/10.1016/j.envpol.2018.07.131.

Dehaut, A., Cassone, A.-L., Frère, L., Hermabessiere, L., Himber, C., Rinnert, E., Rivière, G., Lambert, C., Soudant, P., Huvet, A., Duflos, G., Paul-Pont, I., 2016. Microplastics in seafood: benchmark protocol for their extraction and characterization. Environ. Pollut. 215, 223–233. https://doi.org/10.1016/j.envpol.2016.05.018.

DRM, 2019. Bulletin Statistique - Synthèse des données de la pêche professionnelle, 2019. de l'aquaculture et de la perliculture - Edition.

Enders, K., Lenz, R., Stedmon, C.A., Nielsen, T.G., 2015. Abundance, size and polymer composition of marine microplastics ≥10 μm in the Atlantic Ocean and their modelled vertical distribution. Mar. Pollut. Bull. 100, 70–81. https://doi.org/10.1016/j.marpolbul.2015.09.027.

Eriksen, M., Maximenko, N., Thiel, M., Cummins, A., Lattin, G., Wilson, S., Hafner, J., Zellers, A., Rifman, S., 2013. Plastic pollution in the South Pacific subtropical gyre. Mar. Pollut. Bull. 68, 71–76. https://doi.org/10.1016/j.marpolbul.2012.12.021.

Eriksen, M., Lebreton, L.C.M., Carson, H.S., Thiel, M., Moore, C.J., Borerro, J.C., Galgani, F., Ryan, P.G., Reisser, J., 2014. Plastic pollution in the world's oceans: more than 5 trillion plastic pieces weighing over 250,000 tons afloat at sea. PLoS One 9, 111913. https://doi.org/10.1371/journal.pone.0111913.

Fazey, F.M.C., Ryan, P.G., 2016. Debris size and buoyancy influence the dispersal distance of stranded litter. Mar. Pollut. Bull. 110, 371–377. https://doi.org/10.1016/j.marpolbul.2016.06.039.

Foekema, E.M., De Gruijter, C., Mergia, M.T., van Franeker, J.A., Murk, A.J., Koelmans, A.A., 2013. Plastic in North Sea Fish. Environ. Sci. Technol. 47, 8818–8824. https://doi.org/10.1021/es400931b.

Frère, L., Paul-Pont, I., Rinnert, E., Petton, S., Jaffré, J., Bihannic, I., Soudant, P., Lambert, C., Huvet, A., 2017. Influence of environmental and anthropogenic factors on the composition, concentration and spatial distribution of microplastics: a case study of the Bay of Brest (Brittany, France). Environ. Pollut. 225, 211–222. https://doi.org/10.1016/j.envpol.2017.03.023.

Galloway, T.S., Cole, M., Lewis, C., 2017. Interactions of microplastic debris throughout the marine ecosystem. Nat. Ecol. Evol. 1. https://doi.org/10.1038/s41559-017-0116.

Gardon, T., Reisser, C., Soyez, C., Quillien, V., Le Moullac, G., 2018. Microplastics affect energy balance and gametogenesis in the pearl oyster *Pinctada margaritifera*. Environ. Sci. Technol. 52, 5277–5286. https://doi.org/10.1021/acs.est.8b00168.

Gardon, T., Morvan, L., Huvet, A., Quillien, V., Soyez, C., Le Moullac, G., Le Luyer, J., 2020. Microplastics induce dose-specific transcriptomic disruptions in energy metabolism and immunity of the pearl oyster *Pinctada margaritifera*. Environ. Pollut. 266, 115180 https://doi.org/10.1016/j.envpol.2020.115180.

Green, D.S., Kregting, L., Boots, B., Blockley, D.J., Brickle, P., da Costa, M., Crowley, Q., 2018. A comparison of sampling methods for seawater microplastics and a first

report of the microplastic litter in coastal waters of Ascension and Falkland Islands. Mar. Pollut. Bull. 137, 695–701. https://doi.org/10.1016/j.marpolbul.2018.11.004.
Hidalgo-Ruz, V., Gutow, L., Thompson, R.C., Thiel, M., 2012. Microplastics in the marine environment: a review of the methods used for identification and quantification. Environ. Sci. Technol. 46, 3060–3075. https://doi.org/10.1021/es2031505.
Hyvärinen, A., Oja, E., 2000. Independent component analysis: algorithms and applications. Neural Netw. 13, 411–430. https://doi.org/10.1016/S0893-6080(00)00026-5.
IEOM, 2019. Polynésie française - Rapport annuel 2018 (No. ISSN 1635-2262). Institut d'Émission d'Outre-Mer.
Imhof, H.K., Sigl, R., Brauer, E., Feyl, S., Giesemann, P., Klink, S., Leupolz, K., Löder, M. G.J., Löschel, L.A., Missun, J., Muszynski, S., Ramsperger, A.F.R.M., Schrank, I., Speck, S., Steibl, S., Trotter, B., Winter, I., Laforsch, C., 2017. Spatial and temporal variation of macro-, meso- and microplastic abundance on a remote coral island of the Maldives, Indian Ocean. Mar. Pollut. Bull. 116, 340–347. https://doi.org/10.1016/j.marpolbul.2017.01.010.
Isobe, A., Uchida, K., Tokai, T., Iwasaki, S., 2015. East Asian seas: a hot spot of pelagic microplastics. Mar. Pollut. Bull. 101, 618–623. https://doi.org/10.1016/j.marpolbul.2015.10.042.
Isobe, A., Uchiyama-Matsumoto, K., Uchida, K., Tokai, T., 2017. Microplastics in the Southern Ocean. Mar. Pollut. Bull. 114, 623–626. https://doi.org/10.1016/j.marpolbul.2016.09.037.
Ivar do Sul, J.A., Costa, M.F., 2014. The present and future of microplastic pollution in the marine environment. Environ. Pollut. 185, 352–364. https://doi.org/10.1016/j.envpol.2013.10.036.
Kedzierski, M., Villain, J., Falcou-Préfol, M., Kerros, M.E., Henry, M., Pedrotti, M.L., Bruzaud, S., 2019. Microplastics in Mediterranean Sea: a protocol to robustly assess contamination characteristics. PLoS One 14, 0212088. https://doi.org/10.1371/journal.pone.0212088.
Kim, I.-S., Chae, D.-H., Kim, S.-K., Choi, S., Woo, S.-B., 2015. Factors influencing the spatial variation of microplastics on high-tidal coastal beaches in Korea. Arch. Environ. Contam. Toxicol. 69, 299–309. https://doi.org/10.1007/s00244-015-0155-6.
Kolandhasamy, P., Su, L., Li, J., Qu, X., Jabeen, K., Shi, H., 2018. Adherence of microplastics to soft tissue of mussels: a novel way to uptake microplastics beyond ingestion. Sci. Total Environ. 610–611, 635–640. https://doi.org/10.1016/j.scitotenv.2017.08.053.
Kooi, M., Nes, E.H., van, Scheffer, M., Koelmans, A.A., 2017. Ups and downs in the ocean: effects of biofouling on vertical transport of microplastics. Environ. Sci. Technol. 51, 7963–7971. https://doi.org/10.1021/acs.est.6b04702.
Kukulka, T., Proskurowski, G., Morét-Ferguson, S., Meyer, D.W., Law, K.L., 2012. The effect of wind mixing on the vertical distribution of buoyant plastic debris. Geophys. Res. Lett. 39. https://doi.org/10.1029/2012GL051116.
Kukulka, T., Law, K.L., Proskurowski, G., 2016. Evidence for the influence of surface heat fluxes on turbulent mixing of microplastic marine debris. J. Phys. Oceanogr. 46, 809–815. https://doi.org/10.1175/JPO-D-15-0242.1.
Lassen, C., Hansen, S.F., Magnusson, K., Hartmann, N.B., Jensen, P.R., Nielsen, T.G., Brinch, A., 2015. Microplastics: occurrence, effects and sources of releases to the environment in Denmark. Danish Environmental Protection Agency.
Lattin, G.L., Moore, C.J., Zellers, A.F., Moore, S.L., Weisberg, S.B., 2004. A comparison of neustonic plastic and zooplankton at different depths near the southern California shore. Mar. Pollut. Bull. 49, 291–294. https://doi.org/10.1016/j.marpolbul.2004.01.020.
Lebreton, L., Slat, B., Ferrari, F., Sainte-Rose, B., Aitken, J., Marthouse, R., Hajbane, S., Cunsolo, S., Schwarz, A., Levivier, A., Noble, K., Debeljak, P., Maral, H., Schoeneich-Argent, R., Brambini, R., Reisser, J., 2018. Evidence that the Great Pacific Garbage Patch is rapidly accumulating plastic. Sci. Rep. 8, 4666. https://doi.org/10.1038/s41598-018-22939-w.
Lindeque, P.K., Cole, M., Coppock, R.L., Lewis, C.N., Miller, R.Z., Watts, A.J.R., Wilson-McNeal, A., Wright, S.L., Galloway, T.S., 2020. Are we underestimating microplastic abundance in the marine environment? A comparison of microplastic capture with nets of different mesh-size. Environ. Pollut. 265, 114721 https://doi.org/10.1016/j.envpol.2020.114721.
Liubartseva, S., Coppini, G., Lecci, R., Creti, S., 2016. Regional approach to modeling the transport of floating plastic debris in the Adriatic Sea. Mar. Pollut. Bull. 103, 115–127. https://doi.org/10.1016/j.marpolbul.2015.12.031.
de Lucia, G.A., Caliani, I., Marra, S., Camedda, A., Coppa, S., Alcaro, L., Campani, T., Giannetti, M., Coppola, D., Cicero, A.M., Panti, C., Baini, M., Guerranti, C., Marsili, L., Massaro, G., Fossi, M.C., Matiddi, M., 2014. Amount and distribution of neustonic micro-plastic off the western Sardinian coast (Central-Western Mediterranean Sea). Mar. Environ. Res. 100, 10–16. https://doi.org/10.1016/j.marenvres.2014.03.017.
Luna-Jorquera, G., Thiel, M., Portflitt-Toro, M., Dewitte, B., 2019. Marine protected areas invaded by floating anthropogenic litter: an example from the South Pacific. Aquat. Conserv. Mar. Freshw. Ecosyst. 29, 245–259. https://doi.org/10.1002/aqc.3095.
Lusher, A.L., Burke, A., O'Connor, I., Officer, R., 2014. Microplastic pollution in the Northeast Atlantic Ocean: validated and opportunistic sampling. Mar. Pollut. Bull. 88, 325–333. https://doi.org/10.1016/j.marpolbul.2014.08.023.
Lusher, A.L., Tirelli, V., O'Connor, I., Officer, R., 2015. Microplastics in Arctic polar waters: the first reported values of particles in surface and sub-surface samples. Sci. Rep. 5, 14947. https://doi.org/10.1038/srep14947.
Mathalon, A., Hill, P., 2014. Microplastic fibers in the intertidal ecosystem surrounding Halifax Harbor, Nova Scotia. Mar. Pollut. Bull. 81, 69–79. https://doi.org/10.1016/j.marpolbul.2014.02.018.
Munari, C., Infantini, V., Scoponi, M., Rastelli, E., Corinaldesi, C., Mistri, M., 2017. Microplastics in the sediments of Terra Nova Bay (Ross Sea, Antarctica). Mar. Pollut. Bull. 122, 161–165. https://doi.org/10.1016/j.marpolbul.2017.06.039.
Napper, I.E., Thompson, R.C., 2016. Release of synthetic microplastic plastic fibres from domestic washing machines: effects of fabric type and washing conditions. Mar. Pollut. Bull. 112, 39–45. https://doi.org/10.1016/j.marpolbul.2016.09.025.
Obbard, R.W., 2018. Microplastics in Polar Regions: the role of long range transport. Curr. Opin. Environ. Sci. Health 1, 24–29. https://doi.org/10.1016/j.coesh.2017.10.004.
Pagès, J., Andrefouët, S., Delesalle, B., Prasil, V., 2001. Hydrology and trophic state in Takapoto Atoll lagoon: comparison with other Tuamotu lagoons. Aquat. Living Resour. 14, 183–193. https://doi.org/10.1016/S0990-7440(01)01113-5.
Pan, Z., Guo, H., Chen, H., Wang, S., Sun, X., Zou, Q., Zhang, Y., Lin, H., Cai, S., Huang, J., 2019. Microplastics in the Northwestern Pacific: abundance, distribution, and characteristics. Sci. Total Environ. 650, 1913–1922. https://doi.org/10.1016/j.scitotenv.2018.09.244.
Peeken, I., Primpke, S., Beyer, B., Gütermann, J., Katlein, C., Krumpen, T., Bergmann, M., Hehemann, L., Gerdts, G., 2018. Arctic sea ice is an important temporal sink and means of transport for microplastic. Nat. Commun. 9. https://doi.org/10.1038/s41467-018-03825-5.
Phuong, N.N., Poirier, L., Pham, Q.T., Lagarde, F., Zalouk-Vergnoux, A., 2018. Factors influencing the microplastic contamination of bivalves from the French Atlantic coast: location, season and/or mode of life? Mar. Pollut. Bull. 129, 664–674. https://doi.org/10.1016/j.marpolbul.2017.10.054.
Pivokonsky, M., Cermakova, L., Novotna, K., Peer, P., Cajthaml, T., Janda, V., 2018. Occurrence of microplastics in raw and treated drinking water. Sci. Total Environ. 643, 1644–1651. https://doi.org/10.1016/j.scitotenv.2018.08.102.
PlasticsEurope, 2020. Plastics - the Facts 2020. An analysis of European plastics production, demand and waste data.
Poulain, M., Mercier, M.J., Brach, L., Martignac, M., Routaboul, C., Perez, E., Desjean, M. C., ter Halle, A., 2019. Small Microplastics As a Main Contributor to Plastic Mass Balance in the North Atlantic Subtropical Gyre. Environ. Sci. Technol. 53, 1157–1164. https://doi.org/10.1021/acs.est.8b05458.
Pouvreau, S., Jonquières, G., Buestel, D., 1999. Filtration by the pearl oyster, *Pinctada margaritifera*, under conditions of low seston load and small particle size in a tropical lagoon habitat. Aquaculture 176, 295–314. https://doi.org/10.1016/S0044-8486(99)00102-7.
Qu, X., Su, L., Li, H., Liang, M., Shi, H., 2018. Assessing the relationship between the abundance and properties of microplastics in water and in mussels. Sci. Total Environ. 621, 679–686. https://doi.org/10.1016/j.scitotenv.2017.11.284.
Rocha-Santos, T., Duarte, A.C., 2015. A critical overview of the analytical approaches to the occurrence, the fate and the behavior of microplastics in the environment. TrAC Trends Anal. Chem. 65, 47–53. https://doi.org/10.1016/j.trac.2014.10.011.
Rodier, M., Longo, S., Henry, K., Ung, A., Lo-Yat, A., Darius, H.T., Viallon, J., Beker, B., Delesalle, B., Chinain, M., 2019. Diversity and toxic potential of algal bloom-forming species from Takaroa lagoon (Tuamotu, French Polynesia): a field and mesocosm study. Aquat. Microb. Ecol. 83, 15–34. https://doi.org/10.3354/ame01900.
Rutledge, D.N., Jouan-Rimbaud Bouveresse, D., 2013. Independent components analysis with the JADE algorithm. TrAC Trends Anal. Chem. 50, 22–32. https://doi.org/10.1016/j.trac.2013.03.013.
Song, Y.K., Hong, S.H., Eo, S., Jang, M., Han, G.M., Isobe, A., Shim, W.J., 2018. Horizontal and vertical distribution of microplastics in Korean coastal waters. Environ. Sci. Technol. 52, 12188–12197. https://doi.org/10.1021/acs.est.8b04032.
Sparks, C., 2020. Microplastics in mussels along the coast of Cape Town, South Africa. Bull. Environ. Contam. Toxicol. 104, 423–431. https://doi.org/10.1007/s00128-020-02809-w.
Tamminga, M., Hengstmann, E., Fischer, E.K., 2018. Microplastic analysis in the South Funen Archipelago, Baltic Sea, implementing manta trawling and bulk sampling. Mar. Pollut. Bull. 128, 601–608. https://doi.org/10.1016/j.marpolbul.2018.01.066.
Thomas, Y., Dumas, F., Andréfouët, S., 2016. Larval connectivity of pearl oyster through biophysical modelling; evidence of food limitation and broodstock effect. Estuar. Coast. Shelf Sci. 182, 283–293. https://doi.org/10.1016/j.ecss.2016.03.010.
Thompson, R.C., Olsen, Y., Mitchell, R.P., Davis, A., Rowland, S.J., John, A.W.G., McGonigle, D., Russell, A.E., 2004. Lost at sea: where is all the plastic? Science 304, 838. https://doi.org/10.1126/science.1094559.
Van Cauwenberghe, L., Janssen, C.R., 2014. Microplastics in bivalves cultured for human consumption. Environ. Pollut. 193, 65–70. https://doi.org/10.1016/j.envpol.2014.06.010.
Van Cauwenberghe, L., Vanreusel, A., Mees, J., Janssen, C.R., 2013. Microplastic pollution in deep-sea sediments. Environ. Pollut. 182, 495–499. https://doi.org/10.1016/j.envpol.2013.08.013.
van Sebille, E., Wilcox, C., Lebreton, L., Maximenko, N., Hardesty, B.D., van Franeker, J. A., Eriksen, M., Siegel, D., Galgani, F., Law, K.L., 2015. A global inventory of small floating plastic debris. Environ. Res. Lett. 10, 124006 https://doi.org/10.1088/1748-9326/10/12/124006.
Wang, G., Ding, Q., Hou, Z., 2008. Independent component analysis and its applications in signal processing for analytical chemistry. TrAC Trends Anal. Chem. 27, 368–376. https://doi.org/10.1016/j.trac.2008.01.009.
Wang, T., Zou, X., Li, B., Yao, Y., Zang, Z., Li, Y., Yu, W., Wang, W., 2019. Preliminary study of the source apportionment and diversity of microplastics: taking floating microplastics in the South China Sea as an example. Environ. Pollut. 245, 965–974. https://doi.org/10.1016/j.envpol.2018.10.110.
Wang, Z., Lin, T., Chen, W., 2020. Occurrence and removal of microplastics in an advanced drinking water treatment plant (ADWTP). Sci. Total Environ. 700, 134520 https://doi.org/10.1016/j.scitotenv.2019.134520.

Woodall, L.C., Sanchez-Vidal, A., Canals, M., Paterson, G.L.J., Coppock, R., Sleight, V., Calafat, A., Rogers, A.D., Narayanaswamy, B.E., Thompson, R.C., 2014. The deep sea is a major sink for microplastic debris. R. Soc. Open Sci. 1, 140317 https://doi.org/10.1098/rsos.140317.

Yuan, W., Liu, X., Wang, W., Di, M., Wang, J., 2019. Microplastic abundance, distribution and composition in water, sediments, and wild fish from Poyang Lake, China. Ecotoxicol. Environ. Saf. 170, 180–187. https://doi.org/10.1016/j.ecoenv.2018.11.126.

Zhang, D., Cui, Y., Zhou, H., Jin, C., Yu, X., Xu, Y., Li, Y., Zhang, C., 2020. Microplastic pollution in water, sediment, and fish from artificial reefs around the Ma'an Archipelago, Shengsi, China. Sci. Total Environ. 703, 134768 https://doi.org/10.1016/j.scitotenv.2019.134768.

Zhang, W., Zhang, S., Wang, J., Wang, Y., Mu, J., Wang, P., Lin, X., Ma, D., 2017. Microplastic pollution in the surface waters of the Bohai Sea, China. Environ. Pollut. 231, 541–548. https://doi.org/10.1016/j.envpol.2017.08.058.

Zhao, S., Danley, M., Ward, J.E., Li, D., Mincer, T.J., 2017. An approach for extraction, characterization and quantitation of microplastic in natural marine snow using Raman microscopy. Anal. Methods 9, 1470–1478. https://doi.org/10.1039/C6AY02302A.

Zhu, L., Bai, H., Chen, B., Sun, X., Qu, K., Xia, B., 2018. Microplastic pollution in North Yellow Sea, China: observations on occurrence, distribution and identification. Sci. Total Environ. 636, 20–29. https://doi.org/10.1016/j.scitotenv.2018.04.182.